

# Phytochemical analysis of *Acacia nilotica* and evaluation of its antileishmanial potential

**Rahat Ali**

Jamia Millia Islamia

**Shams Tabrez**

Jamia Millia Islamia

**Fazlur Rahman**

Jamia Millia Islamia

**Abdulaziz Alouffi**

King Abdulaziz City for Science and Technology

**Bader Alshehri**

Majmaah University

**Fahdah Alshammari**

Northern Border University

**Mohammed Alaidarous**

Majmaah University

**Saeed Banawas**

Majmaah University

**Abdul Aziz Dukhyil**

Majmaah University

**Abdur Rub** (✉ [arub@jmi.ac.in](mailto:arub@jmi.ac.in))

Jamia Millia Islamia

---

## Research Article

**Keywords:** Leishmania, *Acacia nilotica*, antileishmanial, drugs, host, infection, in silico

**Posted Date:** January 21st, 2021

**DOI:** <https://doi.org/10.21203/rs.3.rs-120320/v2>

**License:** © ⓘ This work is licensed under a Creative Commons Attribution 4.0 International License.

[Read Full License](#)

---

## Phytochemical analysis of *Acacia nilotica* and evaluation of its antileishmanial potential

Rahat Ali<sup>a</sup>, Shams Tabrez<sup>a</sup>, Fazlur Rahman<sup>a</sup>, Abdulaziz S. Alouffi<sup>b</sup>, Bader Mohammed Alshehri<sup>c</sup>, Fahdah Aayed Alshammari<sup>d</sup>, Mohammed A. Alaidarous<sup>c,e</sup>, Saeed Banawas<sup>c,e,f</sup>, Abdul Aziz Bin Dukhyil<sup>c</sup>, Abdur Rub<sup>a,\*</sup>

<sup>a</sup>Infection and Immunity Lab (414), Department of Biotechnology, Jamia Millia Islamia (A Central University), New Delhi, India-110025, <sup>b</sup>King Abdulaziz City for Science and Technology, Riyadh, KSA, <sup>c</sup>Department of Medical Laboratory Sciences, College of Applied Medical Sciences, Majmaah University, Al Majmaah, 11952, Saudi Arabia. <sup>d</sup>College of Sciences and Literature Microbiology, Northern Border University, KSA, <sup>e</sup>Health and Basic Sciences Research Center, Majmaah University, Al Majmaah, Saudi Arabia, <sup>f</sup>Department of Biomedical Sciences, Oregon State University, Corvallis, OR 97331,

### \*Corresponding authors:

Dr. Abdur Rub

Email I.D. [arub@jmi.ac.in](mailto:arub@jmi.ac.in)

### Abstract:

*Acacia nilotica* is an important medicinal plant, found in Africa, the Middle East, and the Indian subcontinent. Every part of the plant possesses a wide array of biologically-active and therapeutically important compounds and has been used in the traditional system of medicine. We reported the antileishmanial activity of *Acacia nilotica* (*A. nilotica*) bark methanolic extract through *in vitro* assays and dissected the mechanism of its action through *in silico* studies. Bark methanolic extract exhibited anti-promastigote and anti-amastigote potency with IC<sub>50</sub> value of  $19.6 \pm 0.9037$   $\mu$ g/ml and  $77.52 \pm 5.167$   $\mu$ g/ml respectively in time and dose-dependent manner.

It showed very low cytotoxicity having a  $CC_{50}$  value of  $432.7 \pm 7.71 \mu\text{g/ml}$  on the human-macrophage cell line, THP-1. The major constituents identified by GC-MS analysis are 13-docosenoic acid (34.06%), lupeol (20.15 %), 9,12-octadecadienoic acid (9.92 %), and 6-octadecanoic acid (8.43 %) bind effectively with the potential drug-targets of *Leishmania donovani* (*L. donovani*) including sterol 24-c-methyltransferase (SMT), trypanothione reductase (TR), pteridine reductase (PTR1) and adenine phosphoribosyltransferase (APRT); suggest the possible mechanism of its antileishmanial action. The highest affinity with all these targets was shown by lupeol. The pharmacokinetic studies, predicted bioactivity scores, and acute toxicity studies of major extract constituents support safe antileishmanial drug candidates. This study proved the antileishmanial potential of bark-methanolic extract *A. nilotica* and its mechanism of action through the inhibition of potential drug targets of *L. donovani*.

**Keywords:** *Leishmania*; *Acacia nilotica*; antileishmanial, drugs; host; infection; *in silico*

**Running Title:** Antileishmanial potential of *A. nilotica* bark extract

## **1. Introduction:**

Visceral leishmaniasis (VL), also known as Kala-Azar in the Indian subcontinent, is a fatal form of the vector-borne disease caused by protozoan parasites *L. donovani*. The disease remains endemic in more than 60 countries around the globe, while 95 % of cases are concentrated in 7 to 8 countries. More than 50 % of the global burden of VL is found in the Indian subcontinent (India, Bangladesh, and Nepal).<sup>1, 2</sup> The disease is proved to be fatal if left untreated in more than 95 % of cases because of secondary infection and anemia.<sup>3</sup> VL is ranked second in mortality rate among the neglected tropical diseases.<sup>4, 5</sup> It is a significant problem for the economically weaker section of the society. Due to their unhygienic living environment, they are more vulnerable to the disease. Illiteracy is another factor that is directly proportional to the lack of awareness which

leads to major morbidity and mortality. The available chemotherapy of visceral leishmaniasis is limited and undermined by drug resistance. Currently, in general, the drug used in the Indian subcontinent sodium antimony gluconate (SAG) showed no response in more than 64 % of the patients due to the development of resistance against the parasites.<sup>6</sup> Alternate drugs, miltefosine, amphotericin B, and its lipid formulations have several limitations because of high toxicity, cost, and unavailability, limit its use. The present scenario of disease and its limited treatment options demand an urgent need to develop a promising and cost-effective operational drug to overcome the disease. In the case of parasitic disease, directly targeting parasites is found to be significant in disease recovery. To date, large numbers of medicinal plants and their extracts had been studied for antileishmanial activity and proved to be potential therapeutic options.<sup>7, 8</sup> Here, we planned to explore the antileishmanial activity of the medicinal plant, *A. nilotica*. *A. nilotica* is commonly known as babul, belongs to the family Fabaceae of genus Acacia, is an important medicinal plant, found in Africa, the Middle East, and the Indian subcontinent.<sup>9-11</sup> It is rich in secondary metabolites including condensed tannins, flavonoids, gums and phlobatannins.<sup>12, 13</sup> Every part of the plant possess a wide array of biologically active, therapeutically potential compounds that have been used in traditional system of medicine, as a remedy for various diseases. Its different parts are used in the treatment of different diseases like floral parts for gastrointestinal disorders <sup>14</sup>, leaves extracts for cancer and microbial infections <sup>15, 16</sup>, roots extract for tuberculosis and liver disorders <sup>17</sup> bark for bacterial infections including cold, bronchitis, dysentery, biliousness, cholera, bleeding piles.<sup>12, 18-20</sup> The extract of bark contains the different form of tannins ((-) – epigallocatechin-7-gallat, (-) – epigallocatechin-5,7-digallat, dicatechin)<sup>21, 22</sup>, flavonoids ( (+)-catechin-5-gallate, (+)-catechin-5,7-digallate, (+)-catechin-3',5-digallate, (+)-catechin-4',5-digallate, (+)-mollisacacidin, apigenin-6,8-bis-C-β-D-

glucopyranoside (vicenin), leucocyanadin, kaempferol-7-glucoside, acacetin, umbelliferon, caffeic acid, protocatechuic acid and m-catechol.<sup>12, 23, 24</sup> Keeping the rich antimicrobial bioactive collection of bark of *A. nilotica*, in mind, we planned to study its antileishmanial potential here. We also tried to dissect the mechanism of its antileishmanial action through different *in silico* approaches. SMT, TR, PTR1, and APRT are prerequisite enzymes for survival, pathogenicity, and transmission of *L. donovani*. Therefore, we selected these potential drug-targets for molecular docking study of major constituents of bark-extract identified by GC-MS, with these mentioned essential enzymes of *Leishmania*.

## **2. Materials and method**

**2.1 Chemicals:** M199 media, Roswell park memorial institute (RPMI) 1640 media, penicillin-streptomycin antibiotic cocktail, fetal bovine serum (FBS) were purchased from Gibco. HEPES, sodium bicarbonate, and paraformaldehyde were purchased from Sigma Aldrich. Miltefosine, MTT assay reagents, DMSO, and different solvents were procured from Merck. Propidium iodide and Annexin V apoptosis kit were procured from Thermo scientific. All the other chemicals and reagents were purchased from Sigma Aldrich or Merck unless stated otherwise.

### **2.2 Parasites and cell culture:**

The infective strain of *L. donovani* (MHOM/IN/83/AG83) was obtained from Dr. Rentala Madhubala (School of life science JNU, New Delhi; India). THP-1, a human monocytic cell line was procured from the Cell Repository of National Centre for Cell Science, Pune, India. It was further maintained in M199 media. Human monocytic cell line, THP-1 was maintained in RPMI 1640 media supplemented with 10 % FBS and 1 % penicillin-streptomycin antibiotic medium in a humidified environment at 5 % CO<sub>2</sub> and 37<sup>0</sup>C temperature. THP-1 monocytic cell was

differentiated to macrophages by using phorbol myristate acetate (PMA) at a concentration of 20 ng/ml.

### **2.3 Extract preparation and antileishmanial activity:**

*A. nilotica* was collected from natural habitats. Bark identification was done at the National Institute of Science Communication and Information Resources (NISCAIR), New Delhi, India. The selected plant material was washed and air-dried in shade at room temperature. The powdered plant materials were soaked in methanol and placed on the rotary shaker at room temperature for 24 h. The extract was filtered and concentrated using a rotatory evaporator under vacuum at 35°C. The dried plant extract was stored at -20°C until used for bioassay. To evaluate the anti-promastigote potential of *A. nilotica*, stationary phase ( $2 \times 10^6$  cells/ml) promastigotes were incubated with plant extract for 48 h followed by fixing using 1 % paraformaldehyde and counting through hemocytometer at 22°C. Miltefosine a known antileishmanial drug used as positive control. Percent viability was determined using the formula:

$$\% \text{ Viability} = \frac{\text{Average parasite count per ml (treated)}}{\text{Average parasite count per ml (control)}} \times 100$$

50 % inhibitory concentration (IC<sub>50</sub>) at which parasite growth was reduced by 50 % was assessed by GraphPad Prism 7.00, nonlinear regression curve fit.

### **2.5 Cytotoxicity assessment and anti-amastigote evaluation of extract:**

The cytotoxicity of *A. nilotica* on THP-1 differentiated macrophages was assessed by MTT [3-(4,5 dimethyl- thiazol-2-yl)-2,5-diphenyl tetrazolium bromide]. Briefly,  $2 \times 10^6$  THP-1 monocytes were seeded in 96 well tissue culture plate (200 µl/well) in RPMI1640 complete media for 24 h in a CO<sub>2</sub> incubator at 37°C and 5% CO<sub>2</sub>. After treatment to THP-1 differentiated macrophages, freshly prepared 5 mg/ml MTT was added (20 µl/well) with 50 µl of blank media

and further incubated for 2 to 3 h in a CO<sub>2</sub> incubator. Precipitated formazan was dissolved in dimethyl sulfoxide (DMSO) absorbance was recorded at 570 nm in an ELISA plate reader and percent viability was calculated. To determine the effect of *A. nilotica* on the parasite burden of the host macrophages, 0.5 x 10<sup>6</sup> THP-1 cells were seeded on the coverslip, placed in the six-well plates in a CO<sub>2</sub> incubator at 37<sup>0</sup>C. THP-1 macrophages were plated, infected with *L. donovani* at the ratio of 1:10 (macrophages to *Leishmania*) for 48 h then cells were fixed with chilled methanol and parasite counting was performed under the microscope after Giemsa staining. From the different focus, 100 macrophages were counted to determine the parasite burden of the macrophages. Parasite burden in the infection control was considered 100 %, with respect to parasite load in treated samples.

## **2.6 GC-MS analysis of extract:**

GC-MS analysis was performed to identify the secondary metabolites that may be responsible for the antileishmanial efficacy of *A nilotica*. Bark was crushed, powdered, and extracted in methanol and then analyzed on Shimadzu QP2010 armed with a DB-5MS column. The mass spectrums of the sample were produced in an electron impact ionization mode of 70 eV and the phytochemicals were identified after correlation of the recorded mass spectrum with the reference library WILEY8.LIB and NIST14.LIB supplied with the software of the GC-MS system.

## **2.7 Molecular docking studies:**

To begin with structure-based virtual screening and docking, we used various bioinformatics tools, such as PyRx<sup>25</sup>, AutoDock Vina<sup>26</sup>, PyMOL<sup>27</sup>, and BIOVIA Discovery Studio.<sup>28</sup> The online resources used in the retrieval, analysis, and evaluation of the data are the PubChem database and RCSB Protein Data Bank (PDB).<sup>29</sup> The target proteins of *L. donovani* and the

phytochemical compounds were uploaded into the virtual screening program PyRx. The target protein was changed into a macromolecule, which converted the atomic coordinates into pdbqt format. Molecular docking was performed by selecting the grid box around the crystal structures and the rest of the parameters were left as default. AutoDock Vina was used to predicting the binding mode and the best binding affinity of the phytochemicals. The algorithm used by AutoDock Vina is a hybrid scoring function that is inspired by X-score, which accounts for hydrogen bonding, hydrophobic effect, van der Waals forces, and deformation penalty. Besides, for computing, the binding energy AutoDock Vina combines both the conformational preferences of receptor-ligand complex and experimental affinity measurements. The results of molecular docking were screened for binding affinity and then all possible docked conformations were generated for different constituents. After analyzing with PyMOL and Discovery Studio, only those conformations were selected which specifically interact with the active-site residues of *L. donovani* targeted proteins. Discovery Studio was used to analyze detailed interactions and their types including hydrogen bonds, alkyl, pi-alkyl, halogen, and the van der Waals interactions formed between different constituents and the target proteins. The most favorable binding poses of the rutin were analyzed by choosing the lowest free energy of binding ( $\Delta G$ ) and the lowest inhibition constant ( $K_i$ ) which is calculated using the following formula:

$$K_{i\text{pred}} = \text{exponential}^{(\Delta G/RT)}$$

where  $\Delta G$  is binding affinity (kcal/mol), R (gas constant) is  $1.98 \text{ calK}^{-1}\text{mol}^{-1}$ , and T (room temperature) is 298.15 Kelvin.

## 2.8 Sequence analysis, template identification, homology modeling, and receptor and ligand preparation

The protein sequences of trypanothione reductase (XP\_003858222.1) and sterol 24-c-methyltransferase (XP\_003865366.1) from *L. donovani* were retrieved from NCBI. The blastP<sup>30</sup> was performed against Protein Data Bank for the identification of similar templates. The alignment of the query sequences and template sequences was performed using CLUSTAL  $\Omega$ .<sup>31</sup> The crystal structure of trypanothione reductase from *L. infantum* 2.95 Å resolution (PDB id: 2JK6\_A) and X-ray diffracted crystal structure 1.34 Å resolution (PDB id: 5WP4\_A) were used as template structures to model the 3D structures of trypanothione reductase and sterol 24-c-methyltransferase, respectively. PDB was used to retrieve the template structure. Homology modelling was carried out using Modeller 9.24<sup>32</sup> and PyMol was used for the visualization of the 3D structures. The energy minimization was performed using Discovery studio. The PROCHECK program, Ramachandran plots were also used for the assessment of the model.<sup>33</sup> Crystal structures of the Adenine phosphoribosyltransferase and Pteridine reductase proteins were downloaded from PDB [IDs: 1QB7 (APRT) and 2XOX (PTR1)]. The PDB files used for the docking-based virtual screening study were processed by removing water molecules and adding hydrogen atoms. The proteins were finally prepared by Discovery Studio keeping all the parameters at default. The identification of the critical residues of the binding pockets was taken from the native binding pockets of the available crystal structure of proteins, various submitted literature, from their homologous template proteins, and investigation in the mechanism of inhibition. The 3D structure of 9,12-Octadecadienoic acid, 6-Octadecenoic acid, 13-Docosenoic acid, and Lupeol was retrieved from the PubChem database in SDF format. The atomic coordinates of all the ligands were changed to pdbqt set-up using Open Babel GUI, an open-

source chemical toolbox for the interconversion of chemical structures.<sup>34</sup> Universal Force Field (uff) was used for the energy minimization.<sup>35</sup>

## 2.9 Pharmacokinetics studies

The selected ligands were evaluated for their pharmacological profiles by analyzing for Lipinski's rule of violation-5, which was analyzed by Molsoft L.L.C.: Drug-Likeness and molecular property prediction for drug-likeness. (<http://www.molsoft.com/mprop/>) The bioactivity of the selected inhibitors was checked by Molinspiration. (<https://molinspiration.com/cgi-bin/properties>). The successfully screened ligands were further evaluated for ADMET (absorption, distribution, metabolism, excretion, and toxicity) properties by GUSAR<sup>36</sup> and SwissADME database.<sup>37</sup>

## 3. Results:

### 3.1 Antileishmanial activity of *A. nilotica* on *L. donovani* promastigotes:

The growth inhibitory effects of *A. nilotica* bark methanolic extract fraction was assessed against exponentially growing *L. donovani* promastigotes. *A. nilotica* treatment reduced the promastigotes proliferation in a time and dose-dependent manner. Growth kinetics was assessed for seven days; there was a gradual decrease in the promastigote proliferation at all the doses (Figure 1A). The promastigote culture was completely shattered at the dose concentration of 250 and 500  $\mu\text{g/ml}$  of *A. nilotica*, after the three days of treatment. Miltefosine, an established antileishmanial drug rapidly shattered the promastigote parasites *in vitro*. The *Leishmania* promastigotes without any treatment or with 0.5 % DMSO (solvent control), exponentially grow till the 4<sup>th</sup> day of parasites seeding, conforming to no antileishmanial potential of solvent. After 4<sup>th</sup> day of the experimental setup, the culture even in the control and the solvent control was gradually decreased, because of media exhaustion. The  $\text{IC}_{50}$  value of *A. nilotica* on *Leishmania-*

promastigotes was calculated as  $19.6 \pm 0.9037 \mu\text{g/ml}$  and the miltefosine treated positive control has the  $\text{IC}_{50}$  of  $3.118 \pm 0.2395$  (Figure 1B). *A. nilotica* treatment exhibits the morphological changes in the promastigote stage parasites, though at lower doses the parasites retained normal morphology. At the higher concentrations, there is a reduction in size and shortening of flagella. Miltefosine treatment also exhibited similar morphological changes as extract showed at higher doses (Figure 1C).

### **3.2 Growth reversibility assay after extract treatment:**

*A. nilotica*, treated and untreated parasites were washed with PBS after 7 days, and old media was removed and supplemented with fresh media. The samples were further incubated at  $22^{\circ}\text{C}$  for the next 72 h to study the growth reversibility of parasites. Parasites treated with higher doses do not revert though parasites in flasks of lower dose plant-extract treatment show slower growth reversion (Figure 1D). Suppression of growth reversion was observed significant ( $P < 0.001$ ) at  $250 \mu\text{g/ml}$  of *A. nilotica* in comparison to the untreated sample (Figure 1D).

### **3.3 Cytotoxicity and antileishmanial activity of *A. nilotica* on intra-macrophagic amastigotes**

Upon internalization, promastigotes are transformed into the amastigote form inside the parasitophorous vacuoles of macrophages. These amastigote forms of the parasites are non-motile and define the parasite pathogenicity. Thus, being the biologically and clinically relevant form it was important to check the anti-amastigote efficacy of *A. nilotica* methanolic extract. THP-1 differentiated macrophages were parasitized by *L. donovani* promastigotes and treated with different doses of the extract. Plant extract treatment reduced the intra-macrophagic parasites in a dose-dependent manner with an  $\text{IC}_{50}$  value of  $77.52 \pm 5.167 \mu\text{g/ml}$  (Figure 2A). Miltefosine was taken as a positive control (Figure 2A). Cell cytotoxicity ( $\text{CC}_{50}$ ) of *A. nilotica*

methanolic extract was evaluated along with miltefosine as a positive control on THP-1 differentiated macrophages to study its safe dose. THP-1 differentiated macrophages were incubated with different concentrations of extract/miltefosine (0 to 1000  $\mu\text{g/ml}$ ) and the cell viability was assessed using MTT assay. It was observed that *A. nilotica* has the least cytotoxic effect on the viability and morphology of the macrophages with a  $\text{CC}_{50}$  value of  $432.7 \pm 7.71$   $\mu\text{g/ml}$  while miltefosine showed higher toxicity with a  $\text{CC}_{50}$  value of  $8.219 \pm 0.6337$   $\mu\text{g/ml}$  (Figure 2B). A significant reduction in intra-macrophagic parasite count was observed in the micrographs of Giemsa stained infected and extract treated macrophages (Figure 2C).

### **3.4 TLC-bioautography identification and GC-MS analysis of *A. nilotica* bark methanolic extract:**

Plant secondary metabolites present in *A. nilotica* bark methanolic extract fractions that may have been responsible for the observed antileishmanial effects were identified through TLC-bioautography and GC-MS analysis. The total constituents found were 25 (Table 1) out of which the major constituents were 13-docosenoic acid (34.06 %), lupeol (20.15 %), 9,12-octadecadienoic acid (9.92 %), and 6-octadecanoic acid (8.43 %).

### **3.5 Molecular docking of *A. nilotica* methanolic extract of major constituents with potential drug-targets of *L. donovani***

The TR and SMT enzymes were modelled using Modeller 9.24 and the energy minimization was carried out by BIOVIA Discovery studio. The three-dimensional cartoon representation of TR and SMT enzymes is shown in Figure S1A,2A. The models were selected by analyzing their stereochemical quality using the PROCHECK program. The generated models of TR and SMT show a good quality structure having 99.8 % and 99% residues in the allowed regions of the Ramachandran plot respectively (Figure S1B,2B). PDBsum tool was used to analyze and found

that the 3D structure of the enzyme is composed of mixed  $\alpha$ -helices and  $\beta$ -strands ( $\alpha+\beta$ ) secondary structures.<sup>33</sup> The structural topology of TR and SMT showed 5 sheets, 23 strands, 18 helices and 34 beta turns and 2 sheets, 10 strands, 14 helices, and 41 beta turns, respectively (Figure S1C-D, S2C-D). Multiple sequence alignments were performed and Discovery studio was used to find the key residues and regions around the binding cavity of TR and SMT. The active site residues of the SMT, TR, PTR1, and APT enzymes making different numbers of hydrogen bonds as well as hydrophobic bonds with the ligands were also identified. Based on binding affinity Lupeol; 9,12-Octadecadienoic acid; 6-Octadecenoic acid; and 13-Docosenoic acid have binding energies of  $-8.5$  kcal/mol,  $-5.7$  kcal/mol,  $-5.7$  kcal/mol, and  $-5.6$  kcal/mol;  $-8.4$  kcal/mol,  $-4.9$  kcal/mol,  $-4.9$  kcal/mol, and  $-4.7$  kcal/mol;  $-7.9$  kcal/mol,  $-5.3$  kcal/mol,  $-4.4$  kcal/mol, and  $-5.4$  kcal/mol;  $-6.2$  kcal/mol,  $-6.1$  kcal/mol,  $-5.9$  kcal/mol, and  $-5.9$  kcal/mol with SMT, TR, PTR1, and APT enzymes, respectively (Table 2). The binding pattern of lupeol with SMT, TR, PTR1, and APT may hinder the substrate accessibility and its subsequent inhibition as shown in (Figure 3-6A) where the binding energies and inhibition constants are  $-8.5$  kcal/mol,  $-8.4$  kcal/mol,  $-7.9$  kcal/mol,  $-6.2$  kcal/mol, and  $6.25$   $\mu$ M,  $6.12$   $\mu$ M,  $5.81$   $\mu$ M,  $4.56$   $\mu$ M respectively (Table 2). It shows favorable interactions with SMT through two pi-alkyl bonds with Arg347 and Lys351, TR via a pi-alkyl bond with Tyr198, PTR1 by two pi-alkyl bonds with Val83 and Arg88, and APRT through a hydrogen bond with Thr151. (Figure 3-6B). The binding interaction shown by 9,12-Octadecadienoic acid with SMT, TR, PTR1 and APRT, may obstruct the substrate accessibility of these proteins which leads to their subsequent inhibition as shown in (Figure 3-6C) where the binding energies and inhibition constants are  $-5.7$  kcal/mol,  $-4.9$  kcal/mol,  $-5.3$  kcal/mol,  $-6.1$  kcal/mol, and  $4.19$   $\mu$ M,  $3.60$   $\mu$ M,  $3.90$   $\mu$ M,  $4.49$   $\mu$ M, respectively (Table 2). The favorable interactions are shown by 9,12-Octadecadienoic

acid with SMT through a hydrogen bond with Lys198, TR via a hydrogen bond with Gly376, PTR1 by eighteen pi-alkyl bonds with Phe86, Lys87, Ala90, Ala94, Lys156, Ala157, His160, Arg161, and APRT through a hydrogen bond with Arg82. (Figure 3-6D). The binding pattern of 6-Octadecenoic acid with SMT, TR, PTR1, and APRT may lead to their subsequent inhibition by obstructing their substrate accessibility as shown in (Figure 3-6E) where the binding energies and inhibition constants are  $-5.7$  kcal/mol,  $-4.9$  kcal/mol,  $-4.4$  kcal/mol,  $-5.9$  kcal/mol, and  $4.19$   $\mu$ M,  $3.60$   $\mu$ M,  $3.24$   $\mu$ M,  $4.34$   $\mu$ M, respectively (Table 2). The important and favorable interactions shown by 6-Octadecenoic acid with SMT through two pi-alkyl bonds with Lys198, TR via a hydrogen bond with Gly376, PTR1 by a hydrogen bond with Leu92, and APRT through two hydrogen bonds with Arg37 and Arg82. (Figure 3-6F).

The pattern of interaction of 13-Octadecenoic acid with SMT, TR, PTR1, and APRT may lead to their subsequent inhibition by obstructing their substrate accessibility as shown in (Figure 3-6G) where the binding energies and inhibition constants are  $-5.6$  kcal/mol,  $-4.7$  kcal/mol,  $-5.4$  kcal/mol,  $-5.9$  kcal/mol, and  $4.12$   $\mu$ M,  $3.46$   $\mu$ M,  $3.97$   $\mu$ M,  $4.34$   $\mu$ M respectively (Table 2). It shows favorable interactions with SMT through two hydrogen bonds with Lys241 and Gln263, TR via a hydrogen bond with Gly376, PTR1 by twenty pi-alkyl bonds with Val83, Phe86, Lys87, Ala90, Ala94, Lys156, Ala157, His160, and APRT through a hydrogen bond with Arg37 and Ar82. (Figure 3-6H).

### **3.6 Pharmacokinetics studies of *A. nilotica* bark-methanolic extract constituents:**

The pharmacological studies were done for the selected ligands against Adenine phosphoribosyltransferase, Pteridine reductase, trypanothione reductase, and sterol 24-c-methyltransferase proteins for a good oral administration established through the Lipinski rule of five<sup>38</sup>, which was evaluated by Molsoft L.L.C.: Drug-Likeness and molecular property

prediction. Lipinski's "rule of five" is an analytical approach for predicting drug-likeness stating that molecules had Molecular weight (M.W.  $\leq 500$  Da), high lipophilicity expressed as LogP (LogP  $\leq 5$ ), hydrogen bond donors (HBD  $\leq 5$ ), and hydrogen bond acceptors (HBA  $\leq 10$ ) have good absorption or permeation across the cell membrane. Lupeol, 9,12-Octadecadienoic acid, 6-Octadecenoic acid, and 13-Docosenoic acid followed all the parameters of the Lipinski rule of five, except low lipophilicity as observed from Table 2. As per the Lipinski rule of five, violation of one parameter is acceptable for an orally active drug. The absorption percentage (AB%) was calculated using the formula.<sup>39</sup>

$$AB\% = [109 - (0.345 \times \text{TPSA})]$$

It is important to look into the pharmacokinetic properties of the compounds, before animal and clinical studies. To evaluate the biochemical behavior of these compounds inside an organism in respect of absorption, distribution, metabolism, and excretion (ADME), SwissADME database<sup>37</sup> was used to explore the drug-likeness and pharmacokinetics properties of these compounds. The lipophilicity of Lupeol, 9,12-Octadecadienoic acid, 6-Octadecenoic acid, and 13-Docosenoic acid showed LogPo/w value of 4.76, 4.61, 4.73, and 5.65 that indicates high sublingual absorption respectively. Lupeol and 13-Docosenoic acid possess low gastrointestinal absorption and poor water-soluble capability whereas 9,12-Octadecadienoic acid and 6-Octadecenoic acid shows high gastrointestinal absorption as well as moderate water-soluble capability. None of the compounds are permeable to the blood-brain barrier. 9,12-Octadecadienoic acid, 6-Octadecenoic acid, and 13-Docosenoic acid are CYP1A2 inhibitors, which likely to increase the half-life of these compounds and also prevent serious drug interactions. The drug-likeness criteria are qualified by all the ligands with one violation and possess a significant bioavailability score. The results are summarized in Table 3.

The bioactivity prediction of the major constituents of *A. nilotica* bark-methanolic extract was analyzed through molinspiration. The activity was calculated against G-protein coupled receptor-ligand, ion channel modulator, a kinase inhibitor, nuclear receptor ligand, protease inhibitor, and enzyme inhibitor.<sup>40</sup> The interpreted values for bioactivity were as: active (bioactivity score  $\geq 0$ ), moderately active (bioactivity score: between  $-5.0$  to  $0.0$ ), and inactive (bioactivity score  $\leq -5.0$ ).<sup>41</sup> Lupeol, 9,12-Octadecadienoic acid, 6-Octadecenoic acid, and 13-Docosenoic acid were evaluated as active enzyme inhibitors with values 0.52, 0.23, 0.12, and 0.10, respectively. Lupeol and 9,12-Octadecadienoic acid were evaluated as active protease inhibitors as well as ion channel modulators. (Table 4)

The principal aim of predicting acute toxicity is to evaluate undesirable side effects of a compound after single or multiple exposures to an organism via a known administration route (oral, inhalation, subcutaneous, intravenous, or intraperitoneal). GUSAR was used to determine the acute toxicity of the successfully docked compounds. The parameters used by GUSAR to probe compounds based on the prediction of activity spectra for substances algorithm and quantitative neighborhoods of atoms descriptors. The obtained results were compared with SYMYX MDL Toxicity Database to further categorize them based on the Organisation for Economic Co-operation and Development (OECD) chemical classification manual.<sup>36</sup> The criteria used for these compounds to elicit toxicity based upon the administration route when the compound dose is more than 7000 mg/kg for an intravenous route, more than 500,000 mg/kg in case of the oral route, and more than 20,000 mg/kg for intraperitoneal route and subcutaneous database as shown in Table 5. As per the OECD chemical classification 9,12- Octadecadienoic acid, 6-Octadecenoic acid, 13-Docosenoic acid found to be non-toxic and Lupeol is a Class 5 chemical.

#### 4. Discussion:

Plant extracts have promising medicinal properties and are extensively used in the traditional system of medicine due to the presence of many active and leading medicinal.<sup>42</sup> From the previous studies, it has been revealed that many medicinal plants-extracts and their secondary metabolite contents have proven to be efficient and low toxic antileishmanial drug candidates.<sup>43,</sup>

<sup>44</sup> *A. nilotica* which has been identified as potential medicinal plants, are rich in secondary metabolites. Studies based on GC-MS analysis of *A. nilotica* showed the presence of different types of secondary plant metabolites including polyphenols, mainly composed of condensed tannin and phlobatannin in addition to gallic acid, ellagic acid, catechin, epigallocatechin-7-gallate, flavonoids, and gum.<sup>13</sup> Different solvent extracts of the *A. nilotica* had been shown to have antimicrobial activities including anti-bacterial, anti-fungal, anti-viral, and anti-amebic.<sup>18,45,</sup>

<sup>46</sup> We evaluated the antileishmanial potential of *A. nilotica* and identified its secondary metabolite constituents by GC-MS analysis. *A. nilotica* bark methanolic extract repressed the growth of *L. donovani* promastigotes in a time and dose-dependent manner. It induced morphological changes and cytotoxic mode of parasite killing. The cytotoxic mode of the killing of *A. nilotica* maybe because of its richness in phenolic compounds<sup>47</sup> and phenolic acids which cause irreversible changes to the cell membrane.<sup>48</sup> Methanolic extract of the fruit of *A. nilotica* has been reported to have antileishmanial activity with an IC<sub>50</sub> value of 89.38 µg/ml on the *L. major* promastigotes.<sup>49</sup> Here, we for the first time studied the role of *A. nilotica* bark-methanolic extract against the growth and proliferation of *L. donovani* promastigotes and intra-macrophagic amastigotes. The IC<sub>50</sub> value of *A. nilotica* was determined as 19.6 ± 0.9037 µg/ml, which is higher as compared to the IC<sub>50</sub> value of positive control miltefosine as 3.118 ± 0.2395 µg/ml. But the CC<sub>50</sub> value of *A. nilotica* on macrophages was 432.7 ± 7.71 µg/ml, while that of the

miltefosine was  $8.219 \pm 0.6337 \mu\text{g/ml}$ . The plant extract significantly inhibited the growth of the intra-macrophagic form of the parasites. The  $\text{IC}_{50}$  value of the extract on amastigote form was calculated as  $77.52 \pm 5.167 \mu\text{g/ml}$ . *A. nilotica* has found to have low cytotoxic even after having a higher  $\text{IC}_{50}$  value as compare to the miltefosine. So, the higher concentration of *A. nilotica* can be used to inhibit the growth of amastigotes inside macrophages. The major constituents identified through GC-MS analysis were 13-docosenoic acid (34.06%), lupeol (20.15 %), 9,12-octadecadienoic acid (9.92 %) and 6-octadecanoic acid (8.43 %). To dissect the mechanism of antileishmanial activity of *A. nilotica*, we further performed the molecular docking study of major constituents of extract identified by GC-MS, with essential enzymes of *Leishmania* including SMT, TR, PTR1, and APRT. These enzymes play an essential role in parasite growth, survival, virulence, and transmission inside the host. SMT is required for the biosynthesis of ergosterol, the major membrane sterol in *L. donovani*<sup>50</sup>. The enzyme TR follows thiol-redox metabolism to keep trypanothione in reduced form. This antioxidant property of TR is essential for the survival of *L. donovani*.<sup>51</sup> PTR1 catalyzes the reduction of conjugated and non-conjugated pterins such as reduced biopterin to dihydrobiopterin.<sup>52</sup> APRT plays a vital role in purine metabolism by converting 6-aminopurines into 6-oxypurines.<sup>53</sup> Molecular docking results prove that lupeol and 9,12-Octadecadienoic acid possesses higher binding affinity with SMT, TR, PTR1, and APRT as shown in Table 2. Pharmacological studies of these selected inhibitors for the Lipinski rule of 5 indicated violation of only one Lipinski parameter, as shown in Table 3. The pharmacokinetic properties and acute toxicity of lupeol; 9,12-Octadecadienoic acid; 6-Octadecanoic acid and 13-Docosenoic acid have shown relatively low toxicity profile, which means require high doses to evoke a toxic response. The majority of the compounds are non-toxic chemicals whereas lupeol is a Class 5 chemical with very low toxic effects.<sup>54</sup> The

pharmacokinetic attributes are in favor of these compounds to be exploited as promising antileishmanial drug candidates. It had already been reported that lupeol activates the PI3K/Akt pathway which triggers mechanisms responsible for influencing various cell types, including keratinocytes, stimulated cytotoxicity in fibroblasts, and the regulation of various diseases.<sup>55</sup> The lupeol treatment had shown a high imbalance between Th1/Th2 cytokines production and initiation of pro-inflammatory cytokine response as well as the generation of NO in *L. donovani* infected macrophages.<sup>56</sup> It further supports the antileishmanial activity of *A. nilotica* extract. Thus, *in vitro*, molecular docking, pharmacokinetics studies, bioactivity scores, and acute toxicity studies support possible mechanisms of antileishmanial activity of the extract through inhibition of key *Leishmania* enzymes.

### **Acknowledgment**

The authors would like to thank the Deanship of Scientific Research at Majmaah University, Al Majmaah, 11952, Saudi Arabia for supporting this work under the Group Project Number RGP-2019-31. The authors also would like to thank the Ministry of AYUSH (Z. 28015/252/2015-HPC(EMR)-AYUSH-C) GoI for supports. ST is thankful to ICMR, GoI for SRF. RA is thankful to AYUSH, GoI for SRF.

### **Conflict of interest**

The author showed no conflict of interest.

### **Author Contribution**

The study was conceptualized by AR, SB and AABD, ASA; data acquisition and data analysis were performed by ST, RA, and FR; manuscript preparation and manuscript editing were performed by AR, SB, AABD, FR, ASA, BMA, FAA, MAA and ST; the final manuscript was checked by AR and AABD; the fund was obtained by SB, ASA, FAA, MAA, AABD and AR

## References:

1. Murray, H. W.; Berman, J. D.; Davies, C. R.; Saravia, N. G., Advances in leishmaniasis. *Lancet* **2005**, 366 (9496), 1561-77.
2. Huda, M. M.; Hirve, S.; Siddiqui, N. A.; Malaviya, P.; Banjara, M. R.; Das, P.; Kansal, S.; Gurung, C. K.; Naznin, E.; Rijal, S., Active case detection in national visceral leishmaniasis elimination programs in Bangladesh, India, and Nepal: feasibility, performance and costs. *BMC public health* **2012**, 12 (1), 1001.
3. Piscopo, T. V.; Mallia Azzopardi, C., Leishmaniasis. *Postgraduate medical journal* **2007**, 83 (976), 649-57.
4. Global, regional, and national disability-adjusted life-years (DALYs) for 315 diseases and injuries and healthy life expectancy (HALE), 1990-2015: a systematic analysis for the Global Burden of Disease Study 2015. *Lancet* **2016**, 388 (10053), 1603-1658.
5. Wang, H.; Naghavi, M.; Allen, C.; Barber, R. M.; Bhutta, Z. A.; Carter, A.; Casey, D. C.; Charlson, F. J.; Chen, A. Z.; Coates, M. M., Global, regional, and national life expectancy, all-cause mortality, and cause-specific mortality for 249 causes of death, 1980–2015: a systematic analysis for the Global Burden of Disease Study 2015. *The lancet* **2016**, 388 (10053), 1459-1544.
6. Sundar, S., Drug resistance in Indian visceral leishmaniasis. *Tropical medicine & international health : TM & IH* **2001**, 6 (11), 849-54.
7. Chouhan, G.; Islamuddin, M.; Want, M. Y.; Abdin, M. Z.; Ozbak, H. A.; Hemeg, H. A.; Sahal, D.; Afrin, F., Apoptosis mediated leishmanicidal activity of Azadirachta indica bioactive fractions is accompanied by Th1 immunostimulatory potential and therapeutic cure in vivo. *Parasites & vectors* **2015**, 8, 183.
8. Islamuddin, M.; Chouhan, G.; Tyagi, M.; Abdin, M. Z.; Sahal, D.; Afrin, F., Leishmanicidal activities of Artemisia annua leaf essential oil against Visceral Leishmaniasis. *Frontiers in microbiology* **2014**, 5, 626.
9. Hill, A. F., Some nomenclatorial problems in Acacia. *Botanical Museum leaflets, Harvard University* **1940**, 8 (5), 93-105.
10. Bargali, K.; Bargali, S., Acacia nilotica: a multipurpose leguminous plant. *Nature and Science* **2009**, 7 (4), 11-19.
11. Leela, V.; Kokila, L.; Lavanya, R.; Saraswathy, A.; Brindha, P., Determination of gallic acid in Acacia nilotica Linn. by HPTLC. *International Journal of Pharmacy Technology International Journal of Pharmacy Technology* **2010**, 2 (2), 285-292.
12. Singh, B. N.; Singh, B. R.; Singh, R. L.; Prakash, D.; Sarma, B. K.; Singh, H. B., Antioxidant and anti-quorum sensing activities of green pod of Acacia nilotica L. *Food and chemical toxicology : an international journal published for the British Industrial Biological Research Association* **2009**, 47 (4), 778-86.
13. Seigler, D. S. J. B. s.; ecology, Phytochemistry of Acacia—sensu lato. **2003**, 31 (8), 845-873.

14. Gilani, S. A.; Khan, A. M.; Aleem Qureshi, R.; Sherwani, S. K., Ethno-medicinal treatment of common gastrointestinal disorders by indigenous people in Pakistan. *Advances in BioResearch* **2014**, *5* (1), 42-49.
15. Al-Fatimi, M.; Wurster, M.; Schröder, G.; Lindequist, U., Antioxidant, antimicrobial and cytotoxic activities of selected medicinal plants from Yemen. *Journal of ethnopharmacology* **2007**, *111* (3), 657-66.
16. Kalaivani, T.; Mathew, L., Free radical scavenging activity from leaves of *Acacia nilotica* (L.) Wild. ex Delile, an Indian medicinal tree. *Food and chemical toxicology : an international journal published for the British Industrial Biological Research Association* **2010**, *48* (1), 298-305.
17. Eldeen, I.; Van Staden, J., Antimycobacterial activity of some trees used in South African traditional medicine. *South African Journal of Botany* **2007**, *73* (2), 248-251.
18. Bhargava, A.; Srivastava, A.; Kumbhare, V., Antifungal activity of polyphenolic complex of *Acacia nilotica* bark. *Indian forester* **1998**, *124* (5), 292-298.
19. Qasim, M.; Abideen, Z.; Adnan, M. Y.; Ansari, R.; Gul, B.; Khan, M., Traditional ethnobotanical uses of medicinal plants from coastal areas. *J coast life Med* **2014**, *2* (1), 22-30.
20. Baravkar, A.; Kale, R.; Patil, R.; Sawant, S. J. R. J. o. P., Pharmaceutical and biological evaluation of formulated cream of methanolic extract of *Acacia nilotica* leaves. *Research Journal of Pharmacy and Technology* **2008**, *1* (4), 480-483.
21. Hussein Ayoub, S., Flavanol molluscicides from the Sudan Acacias. *International Journal of Crude Drug Research* **1985**, *23* (2), 87-90.
22. Leela, V.; Saraswathy, A., Pharmacognostic studies on the flowers of *Acacia nilotica* Linn. *Pharmacognosy Journal* **2012**, *4* (28), 35-39.
23. Singh, R.; Singh, B.; Singh, S.; Kumar, N.; Kumar, S.; Arora, S., Anti-free radical activities of kaempferol isolated from *Acacia nilotica* (L.) Willd. Ex. Del. *Toxicology in vitro : an international journal published in association with BIBRA* **2008**, *22* (8), 1965-70.
24. Malan, E.; Roux, D. G., Flavonoids and tannins of *Acacia* species. *Phytochemistry* **1975**, *14* (8), 1835-1841.
25. Dallakyan, S.; Olson, A. J., Small-molecule library screening by docking with PyRx. *Methods in molecular biology (Clifton, N.J.)* **2015**, *1263*, 243-50.
26. Trott, O.; Olson, A. J., AutoDock Vina: improving the speed and accuracy of docking with a new scoring function, efficient optimization, and multithreading. *Journal of computational chemistry* **2010**, *31* (2), 455-61.
27. Kashif, M.; Hira, S. K.; Upadhyaya, A.; Gupta, U.; Singh, R.; Paladhi, A.; Khan, F. I.; Rub, A.; Manna, P. P. J. I. j. o. a. a., In silico studies and evaluation of antiparasitic role of a novel pyruvate phosphate dikinase inhibitor in *Leishmania donovani* infected macrophages. **2019**, *53* (4), 508-514.
28. Tabrez, S.; Rahman, F.; Ali, R.; Alouffi, A. S.; Akand, S. K.; Alshehri, B. M.; Alshammari, F. A.; Alam, A.; Alaidarous, M. A.; Banawas, S.; Dukhyil, A. A. B.; Rub, A., Cynaroside inhibits *Leishmania donovani* UDP-galactopyranose mutase and induces reactive oxygen species to exert antileishmanial response. *Bioscience reports* **2020**.
29. Kashif, M.; Tabrez, S.; Husein, A.; Arish, M.; Kalaiarasan, P.; Manna, P. P.; Subbarao, N.; Akhter, Y.; Rub, A., Identification of novel inhibitors against UDP-galactopyranose mutase to combat leishmaniasis. *J Cell Biochem* **2018**, *119* (3), 2653-2665.

30. Kashif, M.; Hira, S. K.; Upadhyaya, A.; Gupta, U.; Singh, R.; Paladhi, A.; Khan, F. I.; Rub, A.; Manna, P. P., In silico studies and evaluation of antiparasitic role of a novel pyruvate phosphate dikinase inhibitor in *Leishmania donovani* infected macrophages. *Int J Antimicrob Agents* **2019**, *53* (4), 508-514.
31. Zimmermann, L.; Stephens, A.; Nam, S. Z.; Rau, D.; Kübler, J.; Lozajic, M.; Gabler, F.; Söding, J.; Lupas, A. N.; Alva, V., A Completely Reimplemented MPI Bioinformatics Toolkit with a New HHpred Server at its Core. *Journal of molecular biology* **2018**, *430* (15), 2237-2243.
32. Sali, A.; Blundell, T. L., Comparative protein modelling by satisfaction of spatial restraints. *Journal of molecular biology* **1993**, *234* (3), 779-815.
33. Laskowski, R. A.; Rullmann, J. A.; MacArthur, M. W.; Kaptein, R.; Thornton, J. M., AQUA and PROCHECK-NMR: programs for checking the quality of protein structures solved by NMR. *Journal of biomolecular NMR* **1996**, *8* (4), 477-86.
34. O'Boyle, N. M.; Banck, M.; James, C. A.; Morley, C.; Vandermeersch, T.; Hutchison, G. R., Open Babel: An open chemical toolbox. *Journal of cheminformatics* **2011**, *3*, 33.
35. Rappé, A. K.; Casewit, C. J.; Colwell, K.; Goddard III, W. A.; Skiff, W. M. J. J. o. t. A. c. s., UFF, a full periodic table force field for molecular mechanics and molecular dynamics simulations. **1992**, *114* (25), 10024-10035.
36. Lagunin, A.; Zakharov, A.; Filimonov, D.; Poroikov, V., QSAR Modelling of Rat Acute Toxicity on the Basis of PASS Prediction. *Molecular informatics* **2011**, *30* (2-3), 241-50.
37. Daina, A.; Michielin, O.; Zoete, V., SwissADME: a free web tool to evaluate pharmacokinetics, drug-likeness and medicinal chemistry friendliness of small molecules. *Sci Rep* **2017**, *7*, 42717.
38. Lipinski, C. A., Lead- and drug-like compounds: the rule-of-five revolution. *Drug discovery today. Technologies* **2004**, *1* (4), 337-41.
39. Zhao, Y. H.; Abraham, M. H.; Le, J.; Hersey, A.; Luscombe, C. N.; Beck, G.; Sherborne, B.; Cooper, I., Rate-limited steps of human oral absorption and QSAR studies. *Pharmaceutical research* **2002**, *19* (10), 1446-57.
40. Mokhnache, K.; Madoui, S.; Khither, H.; Charef, N., Drug-Likeness and Pharmacokinetics of a bis-Phenolic Ligand: Evaluations by Computational Methods. *Sch J App Med Sci* **2019**, *1*, 167-173.
41. Ungell, A.-L., In Vitro Absorption Studies and Their Relevance to Absorption from the GI Tract. *Drug Development and Industrial Pharmacy* **1997**, *23* (9), 879-892.
42. Farnsworth, N. R., The role of ethnopharmacology in drug development. *Ciba Foundation symposium* **1990**, *154*, 2-11; discussion 11-21.
43. Chouhan, G.; Islamuddin, M.; Sahal, D.; Afrin, F., Exploring the role of medicinal plant-based immunomodulators for effective therapy of leishmaniasis. *Frontiers in immunology* **2014**, *5*, 193.
44. Tahir, A. E.; Ibrahim, A. M.; Satti, G. M.; Theander, T. G.; Kharazmi, A.; Khalid, S. A. J. P. R. A. I. J. D. t. P., The potential antileishmanial activity of some Sudanese medicinal plants. *Phytotherapy Research: An International Journal Devoted to Pharmacological and Toxicological Evaluation of Natural Product Derivatives* **1998**, *12* (8), 576-579.
45. Rai, S. P.; Prasad, M. S.; Singh, K., Evaluation of the antifungal activity of the potent fraction of hexane extract obtained from the bark of *Acacia nilotica*. *IJSR* **2014**, *3*, 730-8.
46. Ambasta, S. P., *The Useful Plants of India*. Publication and information Directorate, Council of Scientific & Industrial Research: New Delhi, India, 1994.

47. Sadiq, M. B.; Hanpithakpong, W.; Tarning, J.; Anal, A. K., Screening of phytochemicals and in vitro evaluation of antibacterial and antioxidant activities of leaves, pods and bark extracts of *Acacia nilotica* (L.) Del. *Industrial Crops and Products* **2015**, *77*, 873-882.
48. Borges, A.; Ferreira, C.; Saavedra, M. J.; Simões, M., Antibacterial activity and mode of action of ferulic and gallic acids against pathogenic bacteria. *Microbial drug resistance (Larchmont, N.Y.)* **2013**, *19* (4), 256-65.
49. Fatima, F.; Khalid, A.; Nazar, N.; Abdalla, M.; Mohamed, H.; Toum, A. M.; Magzoub, M.; Ali, M. S., In vitro assessment of anti - cutaneous leishmaniasis activity of some Sudanese plants. *Turkiye parazitoloji dergisi* **2005**, *29* (1), 3-6.
50. Goto, Y.; Bhatia, A.; Raman, V. S.; Vidal, S. E.; Bertholet, S.; Coler, R. N.; Howard, R. F.; Reed, S. G., Leishmania infantum sterol 24-c-methyltransferase formulated with MPL-SE induces cross-protection against L. major infection. *Vaccine* **2009**, *27* (21), 2884-90.
51. Baiocco, P.; Colotti, G.; Franceschini, S.; Ilari, A., Molecular basis of antimony treatment in leishmaniasis. *Journal of medicinal chemistry* **2009**, *52* (8), 2603-12.
52. Ong, H. B.; Sienkiewicz, N.; Wyllie, S.; Fairlamb, A. H., Dissecting the metabolic roles of pteridine reductase 1 in Trypanosoma brucei and Leishmania major. *The Journal of biological chemistry* **2011**, *286* (12), 10429-38.
53. Scotti, L.; Ishiki, H.; Mendonça Júnior, F. J.; Da Silva, M. S.; Scotti, M. T., In-silico analyses of natural products on leishmania enzyme targets. *Mini reviews in medicinal chemistry* **2015**, *15* (3), 253-69.
54. Mielke, H.; Strickland, J.; Jacobs, M. N.; Mehta, J. M., Biometrical evaluation of the performance of the revised OECD Test Guideline 402 for assessing acute dermal toxicity. *Regulatory toxicology and pharmacology : RTP* **2017**, *89*, 26-39.
55. Yu, J. S.; Cui, W., Proliferation, survival and metabolism: the role of PI3K/AKT/mTOR signalling in pluripotency and cell fate determination. *Development (Cambridge, England)* **2016**, *143* (17), 3050-60.
56. Das, A.; Jawed, J. J.; Das, M. C.; Sandhu, P.; De, U. C.; Dinda, B.; Akhter, Y.; Bhattacharjee, S., Antileishmanial and immunomodulatory activities of lupeol, a triterpene compound isolated from Sterculia villosa. *Int J Antimicrob Agents* **2017**, *50* (4), 512-522.

**Figures legends:**

**Figure 1: *A. nilotica* bark methanolic extract inhibits the growth and proliferation of *L. donovani* promastigotes** (A)  $2 \times 10^6$  stationary phase *L. donovani* promastigotes were treated with different concentration of *A. nilotica* methanolic plants extracts, with miltefosine as standard drug and control (without any treatment). Each point is statistically significant as compare to control. (B)  $2 \times 10^6$  stationary phase *L. donovani* promastigotes were treated with different concentration of *A. nilotica* methanolic plant extract fraction and miltefosine,  $IC_{50}$  was determined as described in the methods. Each point represents the mean  $\pm$  SE of the samples in triplicate.(C) Image of the promastigote morphological changes in the treated samples at

different concentration of *A nilotica* fraction and miltefosine treated samples.(D) Stationary phase *L donovani* promastigotes were incubated with different concentration of *A nilotica*, with miltefosine and DMSO (solvent control). And the growth reversal was analyzed as described in methods. \*\*\*P < 0.001 with respect to parasite control. Anti-promastigote efficacy of *A nilotica* fractions.

**Figure 2: *A. nilotica* bark methanolic extract decreases the intra-macrophagic parasites**

(A). Anti-amastigote efficacy determination. THP-1 differentiated macrophages was parasitized in 1:10 ratio with stationary phase promastigotes and then treated with different concentration of *A nilotica* fraction. Percent reduction in the parasite load was determined as described in the method. \*\*\*P < 0.001, value was statistically significant as compare to control.(B).THP-1 differentiated macrophages were treated with different concentration of *A nilotica* and miltefosine (0 to 1000 µg/ml) and cell viability was ascertained by MTT assay. (C). Microscopic *L donovani*infected macrophage images depict parasitized, treated THP-1 differentiated macrophages stained with modified Giemsa stained. The images were captured at 100X under oil immersion. The arrow indicates internalized parasites

**Figure 3: *A. nilotica* major chemical constituents inhibit SMT of *L. donovani* in silico**

(A) Lupeol blocking the binding pocket of SMT enzyme. (B) 2D plot showing interactions between receptor and ligand.(C) 9,12-Octadecadienoic acid blocking the binding pocket of SMT enzyme. (D) 2D plot showing interactions between receptor and ligand. (E) 6-Octadecenoic acid blocking the binding pocket of SMT enzyme. (F) 2D plot showing interactions between receptor and ligand. (G) 13-Docosenoic acid blocking the binding pocket of SMT enzyme. (H) 2D plot showing interactions between receptor and ligand.

**Figure 4: *A. nilotica* major chemical constituents inhibit TR of *L. donovani* in silico**

(A) Lupeol blocking the binding pocket of TR enzyme. (B) 2D plot showing interactions between receptor and ligand. (C) 9,12-Octadecadienoic acid blocking the binding pocket of TR enzyme. (D) 2D plot showing interactions between receptor and ligand. (E) 6-Octadecenoic acid blocking the binding pocket of TR enzyme. (F) 2D plot showing interactions between receptor and ligand. (G) 13-Docosenoic acid blocking the binding pocket of TR enzyme. (H) 2D plot showing interactions between receptor and ligand.

**Figure 5: *A. nilotica* major chemical constituents inhibit PTR1 of *L. donovani* in silico** (A)

Lupeol blocking the binding pocket of PTR1 (PDB ID: 2XOX) enzyme. (B) 2D plot showing interactions between receptor and ligand. (C) 9,12-Octadecadienoic acid blocking the binding pocket of PTR1 (PDB ID: 2XOX) enzyme. (D) 2D plot showing interactions between receptor and ligand. (E) 6-Octadecenoic acid blocking the binding pocket of PTR1 (PDB ID: 2XOX) enzyme. (F) 2D plot showing interactions between receptor and ligand. (G) 13-Docosenoic acid blocking the binding pocket of PTR1 (PDB ID: 2XOX) enzyme. (H) 2D plot showing interactions between receptor and ligand.

**Figure 6: *A. nilotica* major chemical constituents inhibit APRT of *L. donovani* in silico**

(A) Lupeol blocking the binding pocket of APRT (PDB ID: 1QB7) enzyme. (B) 2D plot showing interactions between receptor and ligand. (C) 9,12-Octadecadienoic acid blocking the binding pocket of APRT (PDB ID: 1QB7) enzyme. (D) 2D plot showing interactions between receptor and ligand. (E) 6-Octadecenoic acid blocking the binding pocket of APRT (PDB ID: 1QB7) enzyme. (F) 2D plot showing interactions between receptor and ligand. (G) 13-Docosenoic acid blocking the binding pocket of APRT (PDB ID: 1QB7) enzyme. (H) 2D plot showing interactions between receptor and ligand.

**Tables legends:**

**Table 1:** TLC-bioautography identification and GC-MS analysis of *A. nilotica* bark methanolic extract depicted key chemical constituents of extract

**Table 2:** Molecular docking interaction of abundant medicinal constituents of *A. nilotica* bark methanolic extract shows significant inhibition of *L. donovani* target proteins

**Table 3:** Evaluation of physicochemical and ADMET properties show feasibility of usage of the chemical constituents for the treatment of disease

**Table 4:** Bioactivity prediction of the selected ligands against *L. donovani* by molinspiration

**Table 5:** Acute toxicity shows the lethal dose and extent of toxicity of chemical constituents on rodent models

## Tables

**Table 1: TLC-bioautography identification and GC-MS analysis of *A. nilotica* bark methanolic extract depicted key chemical constituents of extract**

S. NO.	RETENTION TIME	% AREA	COMPOUND IDENTIFIED
1.	13.606	0.45	1H-3A,7-METHANOAZULEN-6-OL
2.	14.220	0.79	1H-BENZOCYCLOHEPTENE
3.	14.290	0.32	PHENOL, 3,5-BIS(1,1-DIMETHYLETHYL)
4.	15.277	1.49	DIETHYL PHTHALATE
5.	16.139	0.54	1-(4-ISOPROPYLPHENYL)-2-METHYLPROPYL ACETATE
6.	18.855	5.42	HEXADECANOIC ACID, METHYL ESTER
7.	19.328	1.71	N-HEXADECANOIC ACID
8.	20.258	0.30	13-HEXYL-OXA-CYCLOTRIDEC-10-EN-2-ONE
9.	<b>20.465</b>	<b>9.92</b>	<b>9,12-OCTADECADIENOIC ACID</b>
10.	20.523	8.43	6-OCTADECENOIC ACID, METHYL ESTER
11.	20.761	2.81	METHYL STEARATE
12.	20.961	1.44	E,E,Z-1,3,12-NONADECATRIENE-5,14-DIOL
13.	22.267	0.17	HEXAHYDRO-3-BUTYLPHTHALIDE
14.	22.311	2.86	CIS-11-EICOSENOIC ACID, METHYL ESTER
15.	22.368	0.53	CIS-13-EICOSENOIC ACID, METHYL ESTER
16.	22.527	1.14	EICOSANOIC ACID, METHYL ESTER
17.	<b>23.965</b>	<b>34.06</b>	<b>13-DOCOSENOIC ACID</b>
18.	24.161	0.84	DOCOSANOIC ACID
19.	25.532	1.52	CIS-15-TETRACOSENSAEURE
20.	25.721	0.70	TETRACOSANOIC ACID
21.	25.897	0.85	CYCLOPENTADECANONE
22.	27.325	0.34	OCTACOSANE
23.	27.885	0.83	9-OCTADECENAL

24.	33.099	2.36	STIGMASTEROL
25.	<b>36.679</b>	<b>20.15</b>	<b>LUPEOL</b>

**Table 2: Molecular docking interaction of abundant medicinal constituents of *A. nilotica* bark methanolic extract shows significant inhibition of *L. donovani* target proteins**

S. No.	Proteins	Ligands	Binding energy (Kcal/mol)	pK <sub>i</sub> <sub>pred</sub> (μM)	Interacting Residues
1.	Sterol 24-c-methyltransferase	Lupeol	-8.5	6.25	Lys198, Tyr206, Met210, Asn215, Pro216, Asn217, Cys240, Gln242, Leu322, Ile344, Arg347, Lys348, Lys351
		9,12-Octadecadienoic acid	-5.7	4.19	<b>Lys198</b> , Cys202, Phe203, Tyr206, Met210, Asn215, Asn217, Cys240, Lys241, Phe259, Gln263, Leu322, Ile344, Arg347, Lys348, Lys351
		6-Octadecenoic acid	-5.7	4.19	<b>Lys198</b> , Cys202, Phe203, Tyr206, Met210, Asn215, Asn217, Cys240, Lys241, Ala257, Phe259, Ile261, Gln263, Leu322, Ile344, Arg347, Lys348, Lys351
		13-Docosenoic acid	-5.6	4.12	Lys198, Gly200, Cys202, Phe203, Tyr206, Met210, Asn215, Pro216, Asn217, <b>Lys241</b> , Phe259, <b>Gln263</b> , Leu322, Ile344, Arg347, Lys348, Lys351
2.	Trypanothione reductase	Lupeol	-8.4	6.12	Gly197, Tyr198, Phe230, Val332, Met333, Leu334, His359, Val362, Cys364, Gly374
		9,12-Octadecadienoic acid	-4.9	3.60	Tyr198, Phe230, Val332, Met333, Cys364, <b>Gly376</b>
		6-Octadecenoic acid,	-4.9	3.60	Gly197, Tyr198, Gly229, Phe230, Val332, Met333, Leu334, Cys362, Cys364, Gly374, Cys375, <b>Gly376</b>

		13- Docosenoic acid	-4.7	3.46	Gly197, Tyr198, Phe230, Gly286, Val332, Met333, Leu334, Lys361, Cys362, Cys364, Gly374, Cys375, <b>Gly376</b>
3.	Pteridine reductase	Lupeol	-7.9	5.81	His38, Gln63, Ala64, Asp65, Lys71, Ala77, Val83, Lys87, Arg88, Asp91
		9,12- Octadecadi enoic acid	-5.3	3.90	Phe86, Lys87, Ala90, Ala94, Lys156, Ala157, His160, Arg161
		6- Octadeceno ic acid	-4.4	3.24	Lys71, Ala77, Val83, Lys87, Arg88, <b>Leu92</b>
		13- Docosenoic acid,	-5.4	3.97	Val83, Phe86, Lys87, Ala90, Ala94, Lys156, Ala157, His160, Arg161
4.	Adenine phosphor ybosyl transferas e	Lupeol	-6.2	4.56	Pro36, Arg37, Arg82, Lys103, Glu127, Asp146, Ala150, <b>Thr151</b> , Glu152, Gly153, Thr154
		9,12- Octadecadi enoic acid	-6.1	4.49	Trp29, Arg37, Val39, Pro40, Arg41, Phe42, Ala43, <b>Arg82</b> , Val148, Ala150, Leu176, Ile178, Leu181, Asp206, Leu209
		6- Octadeceno ic acid	-5.9	4.34	<b>Arg37</b> , Val39, Pro40, Arg41, Phe42, Ala43, <b>Arg82</b> , Val148, Ala150, Leu176, Ile178, Phe180, Leu181, Asp206
		13- Docosenoic acid	-5.9	4.34	<b>Arg37</b> , Val39, Pro40, Arg41, Phe42, Ala43, <b>Arg82</b> , Val148, Ala150, Leu176, Ile178, Phe180, Leu181, Asp206, Leu209

**Table 3: Evaluation of physico-chemical and ADMET properties show feasibility of usage of the chemical constituents for the treatment of disease**

Ligands	MW (<500)	HB D (<5)	HB A (<10)	Log Po/w (Lipophilicity)	TPSA (≤140)	Absorption percentage (AB%) (>50%)	Druglikeness (Lipinski violations)	GI-absorption	BB permeant	CYP 1A2 inhibitor	Bioavailability score	Water solubility (Log S)
Lupeol	426.39	1	1	4.76	20.23	102.02	Yes; 1 violation	Low	No	No	0.55	-8.64 (Poorly Soluble)
9,12-Octadecadienoic acid	294.48	0	2	4.61	26.30	99.93	Yes; 1 violation	High	No	Yes	0.55	-4.97 (Moderately Soluble)
6-Octadecenoic acid	296.50	0	2	4.73	26.30	99.93	Yes; 1 violation	High	No	Yes	0.55	-5.13 (Moderately Soluble)
13-Docosenoic acid	352.60	0	2	5.65	26.30	99.93	Yes; 1 violation	Low	No	Yes	0.55	-6.58 (Poorly Soluble)

**Table 4: Bioactivity prediction of the selected ligands against *L. donovani* by molinspiration**

<b>Ligands</b>	<b>GPC R ligand</b>	<b>Ion channel modulator</b>	<b>Kinase Inhibitor</b>	<b>Nuclear receptor ligand</b>	<b>Protease Inhibitor</b>	<b>Enzyme Inhibitor</b>
Lupeol	0.27	0.11	-0.42	0.85	0.15	0.52
9,12- Octadecadienoic acid	0.15	0.07	-0.20	0.14	0.03	0.23
6-Octadecenoic acid	0.03	-0.03	-0.25	0.06	-0.02	0.12
13-Docosenoic acid	0.07	-0.02	-0.17	0.10	0.07	0.10

**Table 5: Acute toxicity shows the lethal dose and extent of toxicity of chemical constituents on rodent models**

<b>S. No.</b>	<b>Ligands</b>	<b>Rat Oral LD50 (mg/kg)</b>	<b>Rat IV LD50 (mg/kg)</b>	<b>Rat SC LD50 (mg/kg)</b>	<b>Rat IP LD50 (mg/kg)</b>	<b>OECD chemical classification</b>
1.	Lupeol	2888,000	5,867	786,900	1684,000	Class 5
2.	9,12- Octadecadienoic acid	8747,000	309,300	9261,000	4673,000	Non-Toxic
3.	6-Octadecenoic acid	7813,000	381,700	7007,000	3028,000	Non-Toxic
4.	13-Docosenoic acid	9279,000	428,600	1,1160000	5206,000	Non-Toxic



# Figures

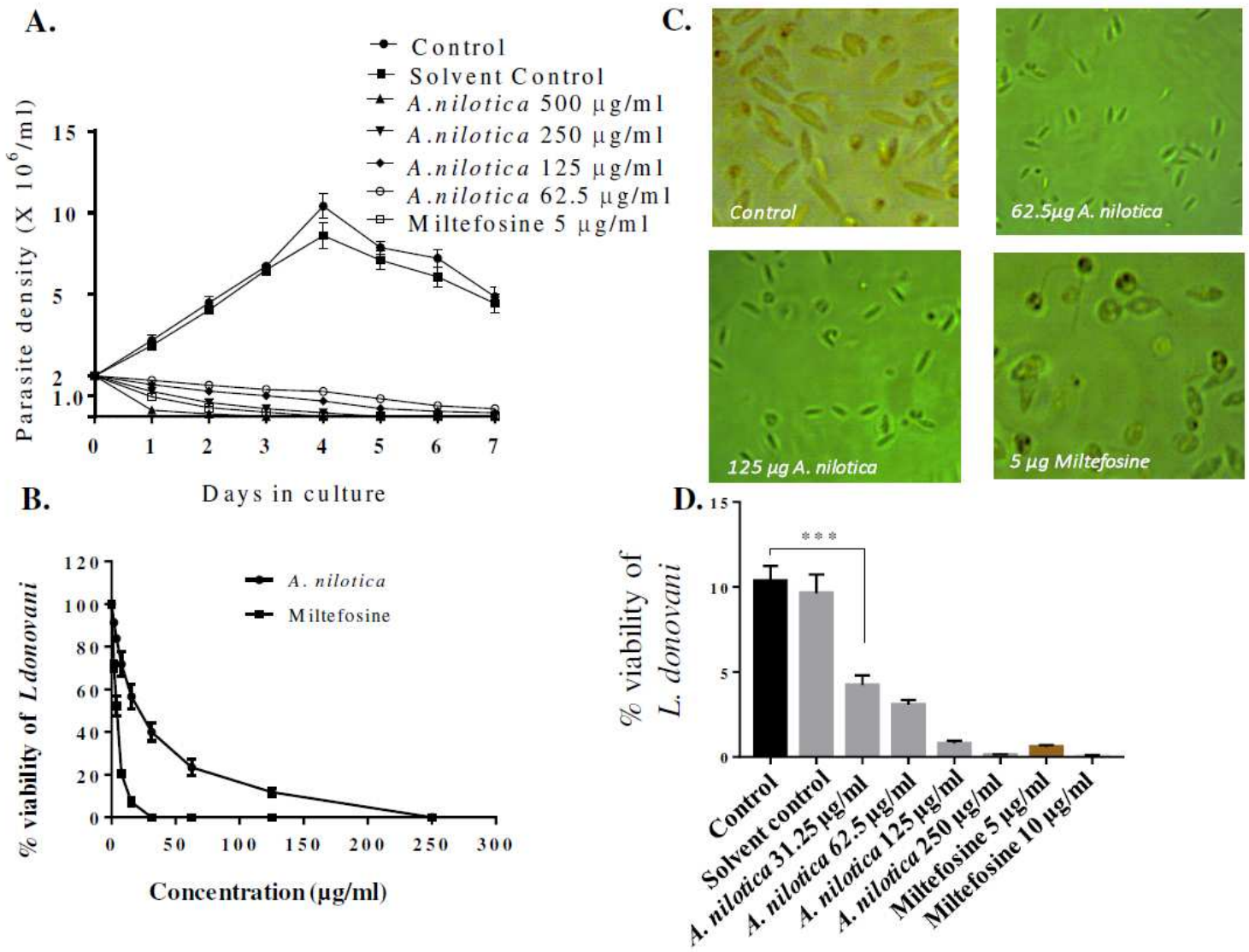


**Figure 1**

*A. nilotica* bark methanolic extract inhibits the growth and proliferation of *L. donovani* promastigotes (A)  $2 \times 10^6$  stationary phase *L. donovani* promastigotes were treated with different concentration of *A. nilotica* methanolic plants extracts, with miltefosine as standard drug and control (without any treatment). Each point is statistically significant as compare to control. (B)  $2 \times 10^6$  stationary phase *L. donovani* promastigotes were treated with different concentration of *A. nilotica* methanolic plant extract fraction and miltefosine, IC50 was determined as described in the methods. Each point represents the mean + SE of the samples in triplicate. (C) Image of the promastigote morphological changes in the treated samples at different concentration of *A. nilotica* fraction and miltefosine treated samples. (D) Stationary phase *L. donovani* promastigotes were incubated with different concentration of *A. nilotica*, with miltefosine and DMSO (solvent control). And the growth reversal was analyzed as described in methods. \*\*\*P < 0.001 with respect to parasite control. Anti-promastigote efficacy of *A. nilotica* fractions.

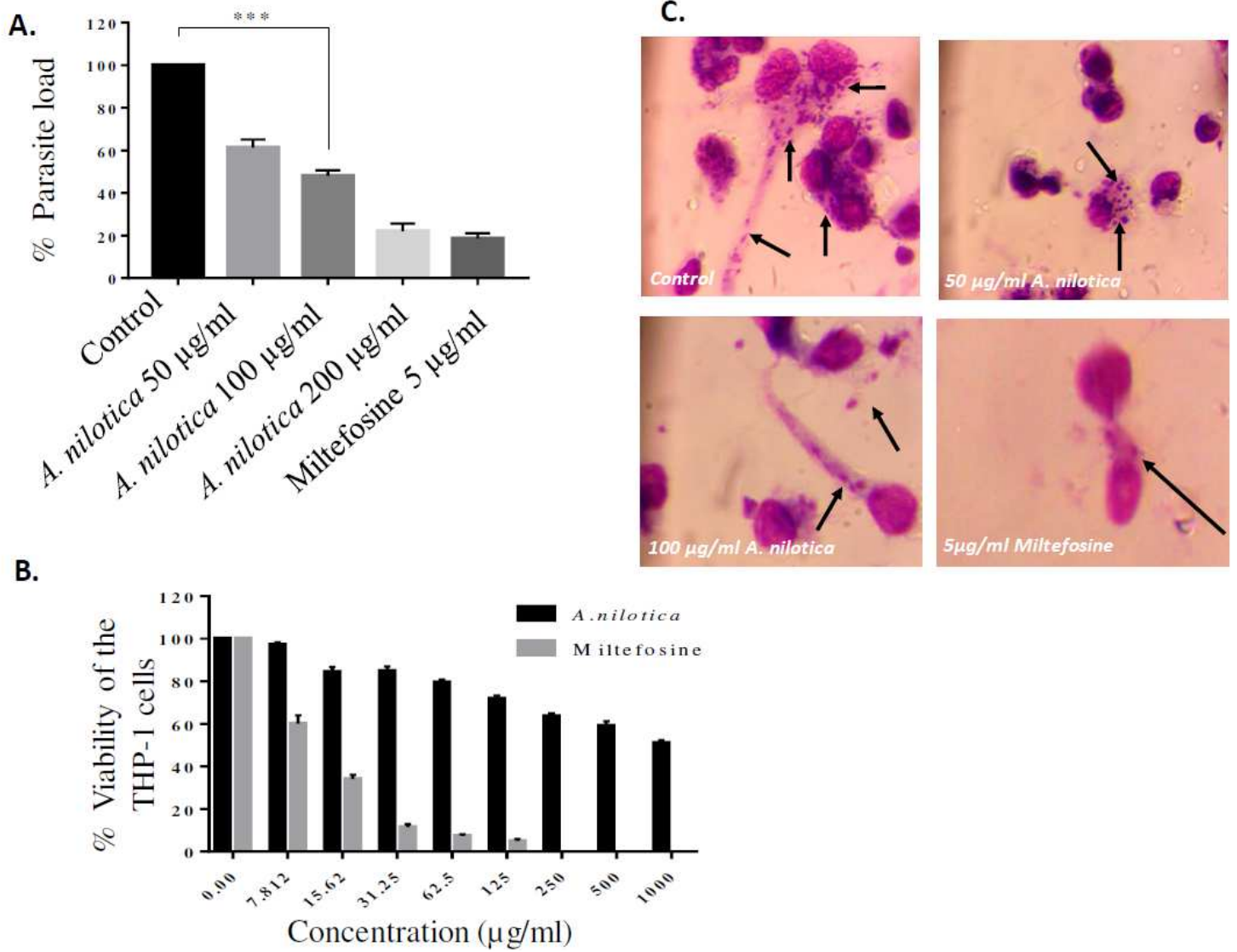


**Figure 2**

*A. nilotica* bark methanolic extract decreases the intra-macrophagic parasites (A). Anti-amastigote efficacy determination. THP-1 differentiated macrophages were parasitized in 1:10 ratio with stationary phase promastigotes and then treated with different concentration of *A. nilotica* fraction. Percent reduction in the parasite load was determined as described in the method. \*\*\* $P < 0.001$ , value was statistically significant as compared to control. (B). THP-1 differentiated macrophages were treated with different concentration of *A. nilotica* and miltefosine (0 to 1000 µg/ml) and cell viability was ascertained by MTT assay. (C). Microscopic *L. donovani*-infected macrophage images depict parasitized, treated THP-1 differentiated macrophages stained with modified Giemsa. The images were captured at 100X under oil immersion. The arrow indicates internalized parasites.

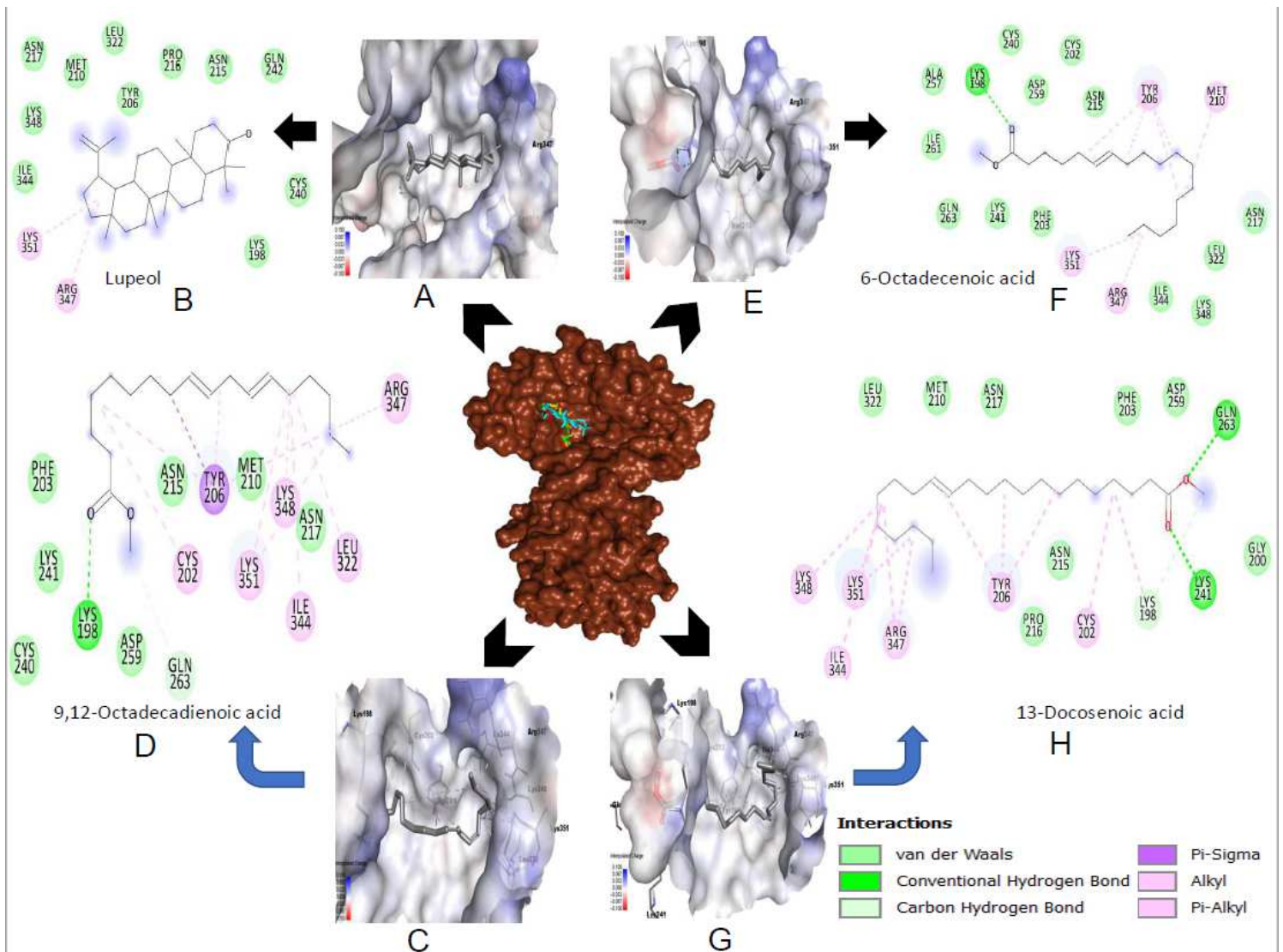


**Figure 3**

A. *nilotica major* chemical constituents inhibit SMT of *L. donovani* in silico (A) Lupeol blocking the binding pocket of SMT enzyme. (B) 2D plot showing interactions between receptor and ligand. (C) 9,12-Octadecadienoic acid blocking the binding pocket of SMT enzyme. (D) 2D plot showing interactions between receptor and ligand. (E) 6-Octadecenoic acid blocking the binding pocket of SMT enzyme. (F) 2D plot showing interactions between receptor and ligand. (G) 13-Docosenoic acid blocking the binding pocket of SMT enzyme. (H) 2D plot showing interactions between receptor and ligand.

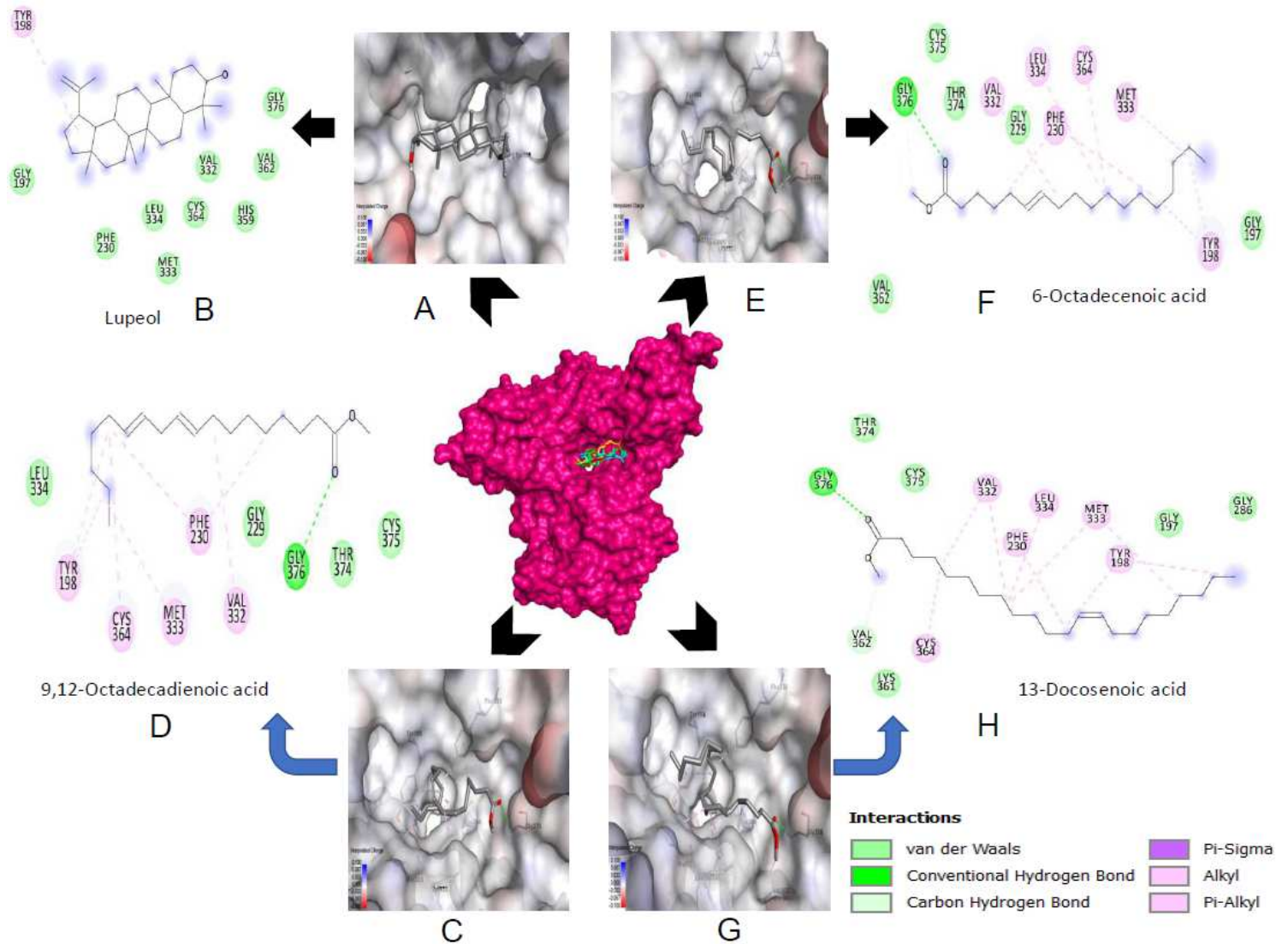


**Figure 4**

A. *nilotica* major chemical constituents inhibit TR of *L. donovani* in silico (A) Lupeol blocking the binding pocket of TR enzyme. (B) 2D plot showing interactions between receptor and ligand. (C) 9,12-Octadecadienoic acid blocking the binding pocket of TR enzyme. (D) 2D plot showing interactions between receptor and ligand. (E) 6-Octadecenoic acid blocking the binding pocket of TR enzyme. (F) 2D plot showing interactions between receptor and ligand. (G) 13-Docosenoic acid blocking the binding pocket of TR enzyme. (H) 2D plot showing interactions between receptor and ligand.

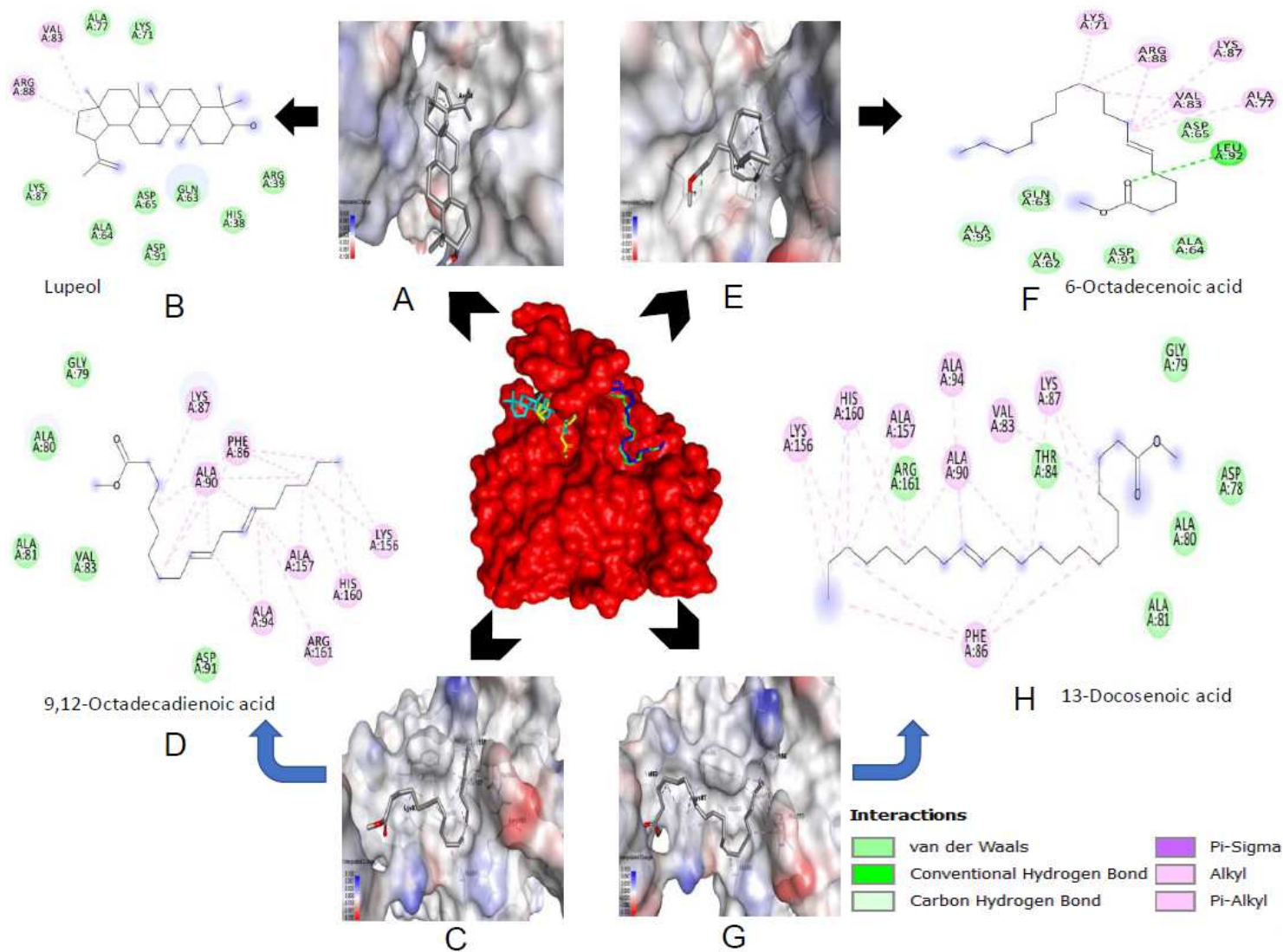


**Figure 5**

A. *nilotica* major chemical constituents inhibit PTR1 of *L. donovani* in silico (A) Lupeol blocking the binding pocket of PTR1 (PDB ID: 2XOX) enzyme. (B) 2D plot showing interactions between receptor and ligand. (C) 9,12-Octadecadienoic acid blocking the binding pocket of PTR1 (PDB ID: 2XOX) enzyme. (D) 2D plot showing interactions between receptor and ligand. (E) 6-Octadecenoic acid blocking the binding pocket of PTR1 (PDB ID: 2XOX) enzyme. (F) 2D plot showing interactions between receptor and ligand. (G) 13-Docosenoic acid blocking the binding pocket of PTR1 (PDB ID: 2XOX) enzyme. (H) 2D plot showing interactions between receptor and ligand.

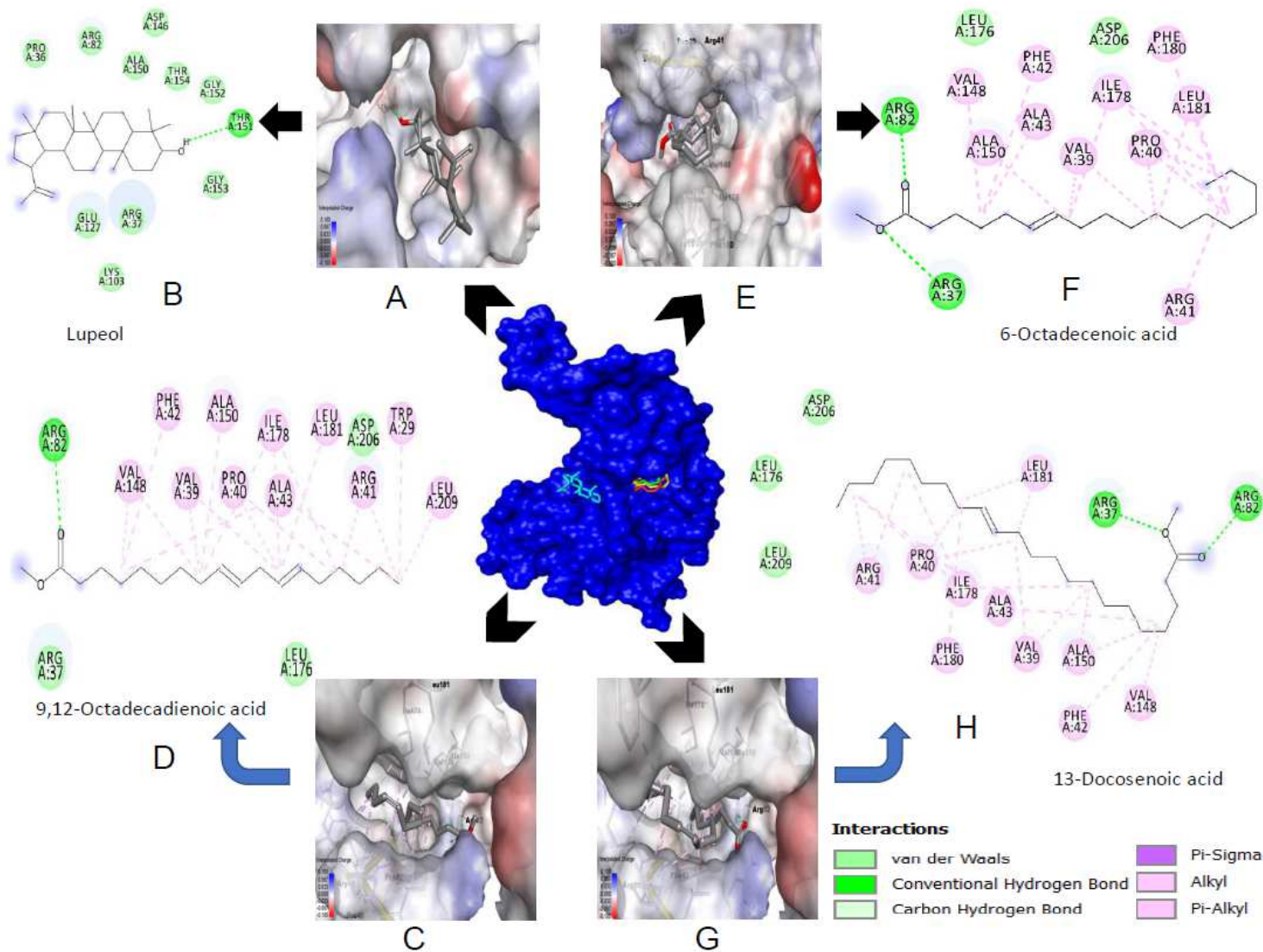


**Figure 6**

A. *nilotica* major chemical constituents inhibit APRT of *L. donovani* in silico (A) Lupeol blocking the binding pocket of APRT (PDB ID: 1QB7) enzyme. (B) 2D plot showing interactions between receptor and ligand. (C) 9,12-Octadecadienoic acid blocking the binding pocket of APRT (PDB ID: 1QB7) enzyme. (D) 2D plot showing interactions between receptor and ligand. (E) 6-Octadecenoic acid blocking the binding pocket of APRT (PDB ID: 1QB7) enzyme. (F) 2D plot showing interactions between receptor and ligand. (G) 13-Docosenoic acid blocking the binding pocket of APRT (PDB ID: 1QB7) enzyme. (H) 2D plot showing interactions between receptor and ligand.

## Supplementary Files

This is a list of supplementary files associated with this preprint. Click to download.

- [SupplementaryMaterials.pdf](#)